



Islam, M. T., Srivastava, P. K., Kumar, D., Petropoulos, G. P., Dai, Q., & Zhuo, L. (2016). Satellite radiance assimilation using a 3DVAR assimilation system for hurricane Sandy forecasts. *Natural Hazards*, 82(2), 845-855. <https://doi.org/10.1007/s11069-016-2221-4>

Peer reviewed version

Link to published version (if available):
[10.1007/s11069-016-2221-4](https://doi.org/10.1007/s11069-016-2221-4)

[Link to publication record on the Bristol Research Portal](#)
PDF-document

The final publication is available at Springer via <http://dx.doi.org/10.1007/s11069-016-2221-4>

University of Bristol – Bristol Research Portal

General rights

This document is made available in accordance with publisher policies. Please cite only the published version using the reference above. Full terms of use are available:
<http://www.bristol.ac.uk/red/research-policy/pure/user-guides/brp-terms/>

Satellite radiance assimilation using a 3DVAR assimilation system for hurricane Sandy forecasts

Tanvir Islam^{*,1,2,3}, Prashant K. Srivastava^{4,5}, Dinesh Kumar⁶, George P. Petropoulos⁷, Qiang Dai⁸, Lu Zhuo⁹

¹ Jet Propulsion Laboratory, California Institute of Technology, Pasadena, CA, USA

² NOAA/NESDIS Center for Satellite Applications and Research, College Park, MD, USA

³ Cooperative Institute for Research in the Atmosphere, Colorado State University, Fort Collins, Colorado, USA

⁴ NASA Goddard Space Flight Center, Greenbelt, MD, USA

⁵ Earth System Science Interdisciplinary Center, University of Maryland, College Park, MD, USA

⁶ Central University of Jammu, Jammu, India

⁷ Department of Geography and Earth Sciences, Aberystwyth University, Aberystwyth, UK

⁸ School of Geographic Science, Nanjing Normal University, Nanjing, China

⁹ Department of Civil Engineering, University of Bristol, Bristol, UK

Submission

Natural Hazards

© 2016. All rights reserved.

***Corresponding author:**

Dr. Tanvir Islam,

NASA Jet Propulsion Laboratory

Earth Science Section (329), M/S 183-518

4800 Oak Grove Drive, Pasadena, CA 91109

Phone: (818) 354 9268, Fax: (818) 354 0988

Email: tanvir.islam@jpl.nasa.gov

ABSTRACT

In this article, we present an assimilation impact study for forecasting hurricane Sandy using a three-dimensional variational data assimilation system (3DVAR). In particular, we employ the 3DVAR component of the Weather Research and Forecasting Model and conduct analysis/forecast cycling experiments for “control” and “radiance” assimilation cases for the hurricane Sandy period. In “control” assimilation experiment, only conventional air and surface observations data are assimilated, while, in “radiance” assimilation experiment, along with the conventional air and surface observations data, the satellite radiance data from the Advanced Microwave Sounding Unit-A (AMSU-A) and the Advanced Microwave Sounding Unit-B (AMSU-B) sensors are also assimilated. For the radiance assimilation, we employ the community radiative transfer model (CRTM) as the forward operator, and perform quality control and bias correction procedure before the radiance data are assimilated. In order to assess the impact of the assimilation experiments, we produce 132 h deterministic forecast starting on 00 UTC 25 October 2012. The results reveal that, in particular, the assimilation of AMSU-A satellite radiances helps to improve the short to medium range forecast (up to ~60 h lead time). The forecast skill is degraded in the long range forecast (beyond 60 h) with the AMSU-A assimilation.

KEYWORDS: variational data assimilation; numerical weather prediction (NWP); cyclone forecast; track propagation; WRF 3DVAR; radiative transfer; ATOVS; AMSU-A, AMSU-B, and MHS;

1. INTRODUCTION

Data assimilation is an active area of research for numerical weather prediction (NWP) model development and day-to-day weather forecasting. The growing advancement of computing power makes it now possible to assimilate large volume of datasets in the operational NWP models. Conventionally, the upper-air and surface meteorological data are assimilated into the NWP models for weather forecasting. However, many places in the earth do not have enough surface and upper-air observations data to be assimilated. Therefore, forecast skills can largely vary from one place to another.

Accurate data assimilation becomes more crucial for extreme weather forecasts, for instance, the forecast of a hurricane that could potentially threat to landfall. In particular, forecasting intensity of a hurricane event has remained one of the challenging tasks to the operational weather forecasters (Islam et al. 2015). Along with hurricane track, if accurate forecast of hurricane intensity can be made, necessary preparation can then be made to save property and lives in timely manner. Prior data assimilation studies have been successful in improving the track and intensity forecast of hurricanes and tropical cyclones. For instances, Subramani et al. (2014) proposed an ensemble based data assimilation algorithm and found better track prediction of tropical cyclones with their algorithm than the control run. Xu and Powell (2012) highlighted that the forecast errors were reduced with the help of satellite radiance data assimilation in the Gridpoint Statistical Interpolation (GSI) system. Xu et al. (2013) investigated the impact of Infrared Atmospheric Sounding Interferometer (IASI) radiance assimilations on the forecasts of two tropical cyclones and confirmed that the depiction of dynamic and thermodynamic vortex structures was improved by the assimilation.

Moreover, research has demonstrated that microwave radiance data has more information in providing vertical profile of sounding observations and inner structure of a hurricane than other satellite measurements. Singh et al. (2012) demonstrated that assimilation of AMSU-A radiances can change the large-scale thermodynamic structure of the atmosphere, and can produce a stronger warmer core than conventional observations assimilation, which are also the cause of large forecast track improvements. Liu et al. (2012) showed that the assimilation of AMSU-A radiance data produced better depictions of the tropical cyclone track and intensity forecasts when compared to reanalyses and dropsonde observations. Additional data assimilation studies can be found in (Chou and Huang 2011), (Jones and Stensrud 2012), (Dong et al. 2013), (Zhang et al. 2013), (Zupanski et al. 2011), (Chambon et al. 2014), among others.

During the 2012 Atlantic hurricane season, the hurricane Sandy has made devastating landfall on the continental US. It was reported as the deadliest and most destructive hurricane in the 2012 Atlantic hurricane season. Excessive economical damages have been reported by the hit of the hurricane Sandy, and lots of lives were lost. This particular hurricane is of interest in this present work. In this study, we examine the impact of assimilating satellite radiance data into an NWP model for the forecasting of track and intensity of the hurricane Sandy. This paper is organized as follows. Section 2 describes the satellite radiance datasets. The 3DVAR assimilation system is introduced in Section 3. Section 4 outlines the experimental setup. Section 5 presents results from the data assimilation studies. Finally, a summary is provided in Section 6.

2. RADIANCE DATA

The Satellite radiance data can be extremely valuable for hurricane forecasting as they provide thermodynamic information over the ocean surface, where hurricane forms. Early studies have confirmed that the temperature sounding information from the Advanced Microwave Sounding

Unit (AMSU-A) instrument to be very valuable for hurricane forecasts (Liu et al. 2012). The use of Microwave Humidity Sounder (MHS) instrument is also found to be very useful in forecasting extreme events (Zou et al. 2013).

The AMSU-A is a cross-track microwave instrument, suited with 15 channels between 23.8 and 89.0 GHz frequencies. It is primarily designed to acquire temperature sounding information from upper atmosphere. Its swath width is 2343 km with a footprint size of around 48 km at nadir. There are a total of 30 fields of views (FOV) per scan line. Each scan takes around 8 sec to complete. On the other hand, the Microwave Humidity Sounder (MHS) is a five channel microwave instrument operating in the 89 to 190 GHz regions. It is also a cross-track sensor that scans three times every eight seconds. This results into a total of 90 pixels across the earth view per scan line. Its swath width is approximately 1920 km. In this article, we assimilate the radiances measured by the AMSU-A and MHS instruments onboard NOAA, and MetopB satellite platforms.

3. 3DVAR ASSIMILATION SYSTEM

3.1. Assimilation methodology

The data assimilation system used in this work is the WRFDA assimilation system developed by the National Center for Atmospheric Research (NCAR). The WRFDA is a unified (global/regional, multi-model, 3/4D-Var) model-space data assimilation system. In this work, we employ the 3DVAR component of the WRFDA system (Barker et al. 2004). More specifically, version 3.6.1 is employed. Mathematically, the 3DVAR assimilation method obtains an optimal estimate of atmospheric state for a given time by minimizing a prescribed cost function $J(x)$:

$$J(x) = \frac{1}{2}(x - x_b)^T B^{-1}(x - x_b) + \frac{1}{2}(y - H(x))^T R^{-1}(y - H(x)) \quad (1)$$

where, x is the state vector composed of atmospheric and surface parameters, x_b is the background vector, y is the observation vector, and H is the non linear observation operator. B is the

background error covariance matrix and R is the observation error covariance matrix. The state vector x is estimated through iterative approach so that the solution designates a minimum variance estimate of the atmospheric state. In order to minimize the cost function, the conjugate gradient method is employed. Readers may refer to the articles of Barker et al. (2004) for a detailed description of the WRF 3DVAR assimilation system.

3.2. Forward operator

In the case of radiance assimilation, a forward operator is used. From Equation 1, H uses a fast radiative transfer model to calculate brightness temperatures from the model variables stored in state vector x . The WRF DA has the capability to use two fast radiative transfer models- the Radiative Transfer for (A)TOVS (RTTOV) model, developed by the EUMETSAT, and the Community Radiative Transfer Model (CRTM), developed by the JCSDA. In the present work, we use the CRTM as the forward operator. The CRTM uses atmospheric temperature and water vapor profiles, surface temperature, surface wind speed, and satellite geometry parameters as inputs to simulate clear sky radiances. The vertical profiles of hydrometeor parameters are required to simulate cloudy radiances. Over ocean, a two-scale emissivity model known as the Fast Microwave Emissivity Model (FASTEM) is used. Over land, a separate land emissivity model is used. The articles appeared in Liu et al. (2013) and Liu and Weng (2013) are worth reading regarding the theory and implementation of the CRTM model.

3.3. Error covariance matrix

In data assimilation, the error covariance matrix plays a crucial role to provide approximate weight between the background and measurements in the analysis. Two different types of background error covariance matrices are available for use in the WRF 3DVAR system. One of them is generated using a global model with T170 resolution by the National Meteorological Center (NMC) method

described in (Wu et al. 2002), known as CV3 default option. The other one is the CV5 option, which uses a regional model for the error covariance matrix generation. The CV3 option is used in this work. In CV3 option, the background error covariances are approximated by averaged 24 hour and 12 hour forecast differences that vary at the same time. The horizontal component of the error is based on the horizontally isotropic and homogeneous recursive filters. On the contrary, vertical component of the error is projected by averaging eigenvectors of the vertical error covariance output. The horizontal and vertical components, both are non-separable.

3.4. Quality control and bias correction

Before assimilating the satellite radiances, quality control step is carried out so that poor observations are not used in the assimilation system.

Table 1 tabulates the characteristics of the AMSU-A and MHS channels. Note that the window channels 1-4 and 15 of AMSU-A can be contaminated from surface. The channels 1-2 of MHS have also contribution from surface. The simulation of window channel radiances can be highly erratic as the background temperature and emissivity are difficult to model and have very large errors. As such, the window channels are not assimilated in this study. In addition, the channels 10-14 of AMSU-A peak above the top boundary of the model. As such, they are also not assimilated. In summary, the AMSU-A channels 5-9 and MHS channels 3-5 are only selected to participate in the assimilation.

Unfortunately, radiance measurements can be heavily biased from those simulated by the forward model. The biases can be introduced by a number of factors. For example, there can be systematic calibration errors in the satellite instruments. The temperature and water vapor profiles used as inputs to the forward model may not be closer to the reality. Additionally, the radiative transfer

model is not perfect, and certainly has its own limitations. Nevertheless, prior to assimilating satellite radiance data, it is necessary to remove the possible biases from the measurements. In particular, the first guess departure, that is the difference between the observation (O) and the first guess (B) should not be biased. In this study, the biases are corrected using a variational bias correction scheme, known as VarBC.

3.5. Forecast model

The forecast model implemented in this work is the WRF ARW dynamic solver (version 3.6.1). The description and applications of the WRF ARW dynamic solver is well established in the literature, and thus referred therein (Skamarock and Klemp 2008; Dai et al. 2013; Ishak et al. 2013; Islam et al. 2013; Srivastava et al. 2013; Islam et al. 2014). Briefly speaking, it is a fully compressible non-hydrostatic primitive equation model that uses a terrain following hydrostatic pressure vertical coordinates. The vertical coordinate η is defined as:

$$\eta = \frac{P_h - P_{top}}{P_{hs} - P_{top}} \quad (2)$$

where, p_{top} is the pressure at the top of the domain, p_h is the hydrostatic component of the pressure normalized by its surface value p_{hs} . The η value is ranged between 0 and 1. The horizontal grid is based on the Arakawa-C grid staggering. The 3rd order Runge-Kutta timestep option is used in the solver. The WRF ARW is capable of using different physics parameterization schemes. Summarizing, the WRF Single-Moment 5-class microphysics scheme (Hong et al. 2004), the Yonsei University planetary boundary layer scheme (Hong et al. 2006), the Grell-3 cumulus parameterization scheme, the Rapid Radiative Transfer Model for longwave radiation, Goddard shortwave for shortwave radiation, MM5 similarity for surface layer physics, and Noah Land Surface Model for land surface physics (Chen and Dudhia 2001) are used in this study.

4. EXPERIMENT SETUP

In this experiment, two nested domains are configured over the vicinity of the hurricane sandy. The domain configuration is visualized in Figure 1. The outer domain covers 182 x 231 grid points with 25 km horizontal resolution. The inner domain is occupied with 356 x 831 grid points with 5 km horizontal resolution. The vertical resolution is set to 28 eta levels.

Three experimental runs are carried out during the period of hurricane Sandy in late October 2012. In the first experimental run, that is the control run (“Control”), the major conventional meteorological observations data are assimilated. Table 2 accumulates the datasets assimilated for the “Control” experimental run. In the second experimental run, along with the above conventional observations, AMSU-A radiance data are also assimilated, from the onboard NOAA and MetopB satellites (hereinafter, denoted as Rad1 experimental run). Finally, third experimental run also includes the assimilation of MHS radiance data, in addition to those assimilated in Rad1 (hereinafter, denoted as Rad2 experimental run).

Figure 2 demonstrates the experimental setup for the Control, Rad1, and Rad2 runs. The cycled forecast-analysis experiments are carried out from 00 UTC 21 October 2012 to 00 UTC 25 October 2012. The model is initialized on 00 UTC 21 October 2012 using NCEP forecast data. The assimilation cycles are kept to every 6 hours, while the 6-h forecast has been used as the first guess. The WRF model boundary conditions have been updated every 6-hr using NCEP 1 x 1 degree resolution forecast data. The WRF 132 h forecast on 00 UTC 25 October 2012 is of interest for this particular study, as the landfall was observed in this period. Note that, during analysis, the raw radiance data are thinned using 120 km thinning mesh avoiding potential correlations between adjacent observations. Given an example, Figure 3 illustrates a snapshot of AMSU-A channel 5

radiance data assimilated on 1800 UTC 21 October 2012, after applying the thinning, quality control, and bias correction procedures.

5. RESULTS

In this section, we provide the results for the hurricane Sandy forecasts from the three experiments. The forecast performance has been evaluated by comparing the model outputs to the best track data. Note that the best track data are obtained from the Atlantic hurricane database developed by the National Hurricane Center (NHC) in Miami, Florida.

In Figure 4 (left), we provide the forecast tracks of the hurricane Sandy for the three assimilation experiments. The best track forecast is also overlaid in the figure for comparison. This forecast is particularly given on 00 UTC 25th October 2012 to 132 h forecast lead-time. During the forecast period, the hurricane has also hit the east coast of the United States yielding landfalls. From the figure, it is quite apparent that the vortex positions of the hurricane during the early forecast periods are quite close to the best track observations. The forecast deviates significantly with respect to the forecast time.

For a detailed assessment, we calculate the absolute track errors for the three assimilation experiments, and plot them as a function of forecast hour in Figure 4 (right). Notably, the forecast track errors follow the similar error trends for the three experiments. In particular, prior to 60 h forecast period, the track error stays approximately below 150 km. Beyond 60 h, the forecast error rises significantly, and have reached around 700 km and above. If we look into detail, the forecast track from the Rad1 experiment agrees more closely with the best track data than other two experiments during the 60 h forecast period. In other words, the assimilation of the AMSU-A channels has helped to minimize the forecast errors as compared to the control run. Nevertheless,

beyond 60 h, the Rad1 experiment based forecast tends to intensify the track errors, and performs poorly as compared to the Control and Rad2 experiments. Summarizing, the positive impact of AMSU-A assimilation is more pronounced in short to medium range forecast (up to ~60 h lead time) than that of long range forecast (beyond 60 h).

Similarly, we plot the forecasted minimum sea level pressure (MSLP) and maximum wind speed as a function of forecast lead time in Figure 5. Eventually, the benefit of the radiance assimilation in MSLP forecast is evident for short lead time (<60 h). That means, by this time, the MSLP for Rad1 and Rad2 experiments are closer to the best track data as compared to the Control experiment. Beyond this lead-time, such improvement of hurricane intensity forecast due to radiance assimilation is not noticeable. This highlights that the gain by assimilating satellite radiances is mainly achieved in short lead forecast in our experimental setup.

6. CONCLUSIONS

This study concentrates on the data assimilation using the WRF 3DVAR assimilation system for the hurricane Sandy forecasts. By using the WRF 3DVAR system, the control and radiance assimilation experiments were made for 132 h forecasts starting at 00 UTC 25th October 2012 during the hurricane Sandy event. In the control forecast, only conventional air and surface observations data were assimilated. However, in the radiance assimilation experiment, the AMSU-A and/or AMSU-B satellite radiance data were also assimilated. Of course, before assimilating satellite radiances, necessary “quality control and bias correction” steps were carried out in order to minimize the systematic differences of satellite radiances between the observed and radiative transfer simulated data. The results of the study reveal that the assimilation of AMSU-A satellite radiances improved the short to medium range forecast. However, negative impact was noticed for the long range forecast (beyond 60 h) with the AMSU-A assimilation.

ACKNOWLEDGEMENTS

Portion of the research was carried out at the Jet Propulsion Laboratory, California Institute of Technology, under a contract with the National Aeronautics and Space Administration (NASA). The data for this study are from NOAA's National Operational Model Archive and Distribution System (NOMADS) which is maintained at NOAA's National Climatic Data Center (NCDC). The views expressed here are those of the authors solely and do not constitute a statement of policy, decision, or position on behalf of NOAA, NASA, or the authors' affiliated institutions.

REFERENCES

- Barker DM, Huang W, Guo YR, Bourgeois AJ, Xiao QN (2004) A three-dimensional variational data assimilation system for MM5: Implementation and initial results. *Mon Weather Rev* 132 (4):897-914. doi:10.1175/1520-0493(2004)132<0897:atvdas>2.0.co;2
- Chambon P, Zhang SQ, Hou AY, Zupanski M, Cheung S (2014) Assessing the impact of pre-GPM microwave precipitation observations in the Goddard WRF ensemble data assimilation system. *Q J R Meteorol Soc* 140 (681):1219-1235. doi:10.1002/qj.2215
- Chen F, Dudhia J (2001) Coupling an advanced land surface-hydrology model with the Penn State-NCAR MM5 modeling system. Part I: Model implementation and sensitivity. *Mon Weather Rev* 129 (4):569-585. doi:10.1175/1520-0493(2001)129<0569:caalsh>2.0.co;2
- Chou CB, Huang HP (2011) The Impact of Assimilating Atmospheric Infrared Sounder Observation on the Forecast of Typhoon Tracks. *Adv Meteorol*:10. doi:10.1155/2011/803593
- Dai Q, Han DW, Rico-Ramirez MA, Islam T (2013) The impact of raindrop drift in a three-dimensional wind field on a radar-gauge rainfall comparison. *Int J Remote Sens* 34 (21):7739-7760. doi:10.1080/01431161.2013.826838

- Dong HP, Li XW, Guo WD, Gao TC (2013) A STUDY ON SATELLITE DATA ASSIMILATION WITH DIFFERENT ATOVS IN TYPHOON NUMERICAL EXPERIMENTS. *J Trop Meteorol* 19 (3):242-252
- Hong SY, Dudhia J, Chen SH (2004) A revised approach to ice microphysical processes for the bulk parameterization of clouds and precipitation. *Mon Weather Rev* 132 (1):103-120. doi:10.1175/1520-0493(2004)132<0103:aratim>2.0.co;2
- Hong SY, Noh Y, Dudhia J (2006) A new vertical diffusion package with an explicit treatment of entrainment processes. *Mon Weather Rev* 134 (9):2318-2341. doi:10.1175/mwr3199.1
- Ishak A, Remesan R, Srivastava P, Islam T, Han DW (2013) Error Correction Modelling of Wind Speed Through Hydro-Meteorological Parameters and Mesoscale Model: A Hybrid Approach. *Water Resour Manag* 27 (1):1-23. doi:10.1007/s11269-012-0130-1
- Islam T, Rico-Ramirez MA, Han DW, Bray M, Srivastava PK (2013) Fuzzy logic based melting layer recognition from 3 GHz dual polarization radar: appraisal with NWP model and radio sounding observations. *Theor Appl Climatol* 112 (1-2):317-338. doi:10.1007/s00704-012-0721-z
- Islam T, Rico-Ramirez MA, Han DW, Srivastava PK (2014) Sensitivity associated with bright band/melting layer location on radar reflectivity correction for attenuation at C-band using differential propagation phase measurements. *Atmos Res* 135:143-158. doi:10.1016/j.atmosres.2013.09.003
- Islam T, Srivastava PK, Rico-Ramirez MA, Dai Q, Gupta M, Singh SK (2015) Tracking a tropical cyclone through WRF-ARW simulation and sensitivity of model physics. *Nat Hazards* 76 (3):1473-1495. doi:10.1007/s11069-014-1494-8
- Jones TA, Stensrud DJ (2012) Assimilating AIRS Temperature and Mixing Ratio Profiles Using an Ensemble Kalman Filter Approach for Convective-Scale Forecasts. *Weather Forecast* 27 (3):541-564. doi:10.1175/waf-d-11-00090.1

- Liu QH, Weng FZ (2013) Using Advanced Matrix Operator (AMOM) in Community Radiative Transfer Model. *IEEE J Sel Top Appl Earth Observ Remote Sens* 6 (3):1211-1218.
doi:10.1109/jstars.2013.2247026
- Liu QH, Xue Y, Li C (2013) Sensor-based clear and cloud radiance calculations in the community radiative transfer model. *Appl Optics* 52 (20):4981-4990. doi:10.1364/ao.52.004981
- Liu ZQ, Schwartz CS, Snyder C, Ha SY (2012) Impact of Assimilating AMSU-A Radiances on Forecasts of 2008 Atlantic Tropical Cyclones Initialized with a Limited-Area Ensemble Kalman Filter. *Mon Weather Rev* 140 (12):4017-4034. doi:10.1175/mwr-d-12-00083.1
- Singh R, Kishtawal CM, Pal PK, Joshi PC (2012) Improved tropical cyclone forecasts over north Indian Ocean with direct assimilation of AMSU-A radiances. *Meteorol Atmos Phys* 115 (1-2):15-34. doi:10.1007/s00703-011-0165-5
- Skamarock WC, Klemp JB (2008) A time-split nonhydrostatic atmospheric model for weather research and forecasting applications. *J Comput Phys* 227 (7):3465-3485.
doi:10.1016/j.jcp.2007.01.037
- Srivastava PK, Han DW, Ramirez MAR, Islam T (2013) Comparative assessment of evapotranspiration derived from NCEP and ECMWF global datasets through Weather Research and Forecasting model. *Atmos Sci Lett* 14 (2):118-125. doi:10.1002/asl2.427
- Subramani D, Chandrasekar R, Ramanujam KS, Balaji C (2014) A new ensemble-based data assimilation algorithm to improve track prediction of tropical cyclones. *Nat Hazards* 71 (1):659-682. doi:10.1007/s11069-013-0942-1
- Wu WS, Purser RJ, Parrish DF (2002) Three-dimensional variational analysis with spatially inhomogeneous covariances. *Mon Weather Rev* 130 (12):2905-2916. doi:10.1175/1520-0493(2002)130<2905:tdvaws>2.0.co;2

- Xu DM, Liu ZQ, Huang XY, Min JZ, Wang HL (2013) Impact of assimilating IASI radiance observations on forecasts of two tropical cyclones. *Meteorol Atmos Phys* 122 (1-2):1-18. doi:10.1007/s00703-013-0276-2
- Xu JJ, Powell AM (2012) Dynamical downscaling precipitation over Southwest Asia: Impacts of radiance data assimilation on the forecasts of the WRF-ARW model. *Atmos Res* 111:90-103. doi:10.1016/j.atmosres.2012.03.005
- Zhang SQ, Zupanski M, Hou AY, Lin X, Cheung SH (2013) Assimilation of Precipitation-Affected Radiances in a Cloud-Resolving WRF Ensemble Data Assimilation System. *Mon Weather Rev* 141 (2):754-772. doi:10.1175/mwr-d-12-00055.1
- Zou XL, Qin ZK, Weng FZ (2013) Improved Quantitative Precipitation Forecasts by MHS Radiance Data Assimilation with a Newly Added Cloud Detection Algorithm. *Mon Weather Rev* 141 (9):3203-3221. doi:10.1175/mwr-d-13-00009.1
- Zupanski D, Zhang SQ, Zupanski M, Hou AY, Cheung SH (2011) A Prototype WRF-Based Ensemble Data Assimilation System for Dynamically Downscaling Satellite Precipitation Observations. *J Hydrometeorol* 12 (1):118-134. doi:10.1175/2010jhm1271.1

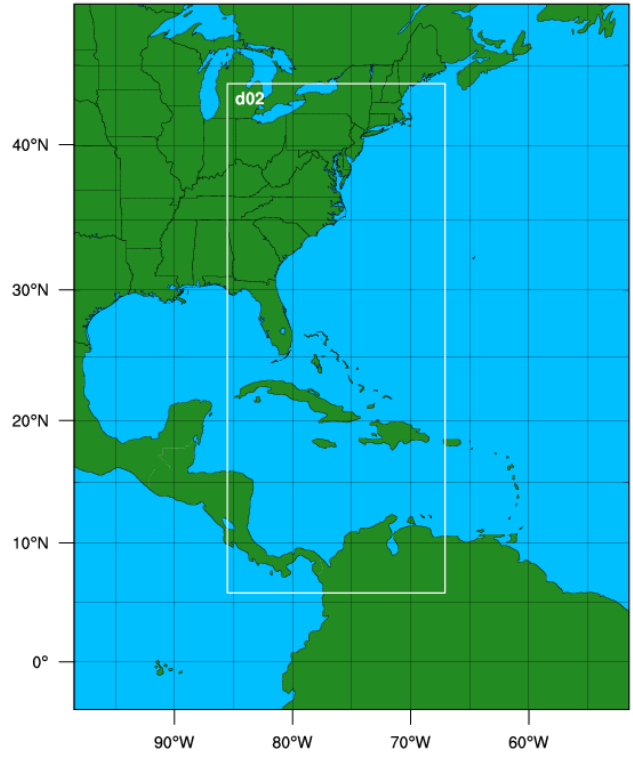


Figure 1: The domain configuration used in this study for the WRF 3DVAR assimilation system.

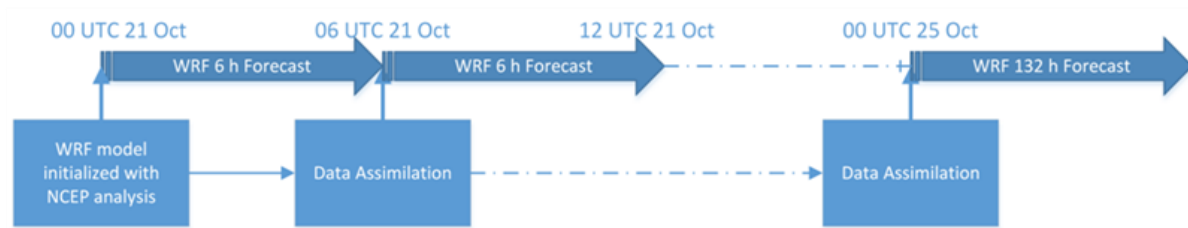


Figure 2: The experimental setup of the data assimilation study and the hurricane Sandy forecast.

noaa-18-amsua_ch0005 OBS 766 / 3083
2012102118

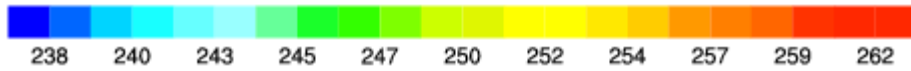
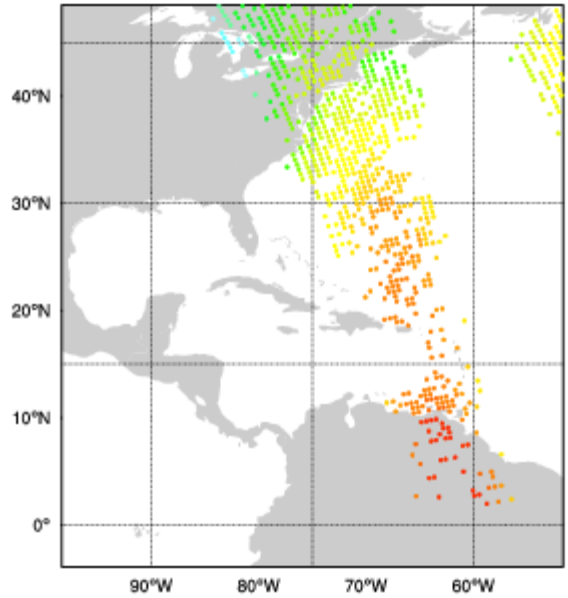


Figure 3: An example illustrating the snapshot of satellite radiance data assimilated on 1800 UTC 21 October 2012. The snapshot is shown for AMSU/A channel 5 after applying the thinning, quality control, and bias correction procedures.

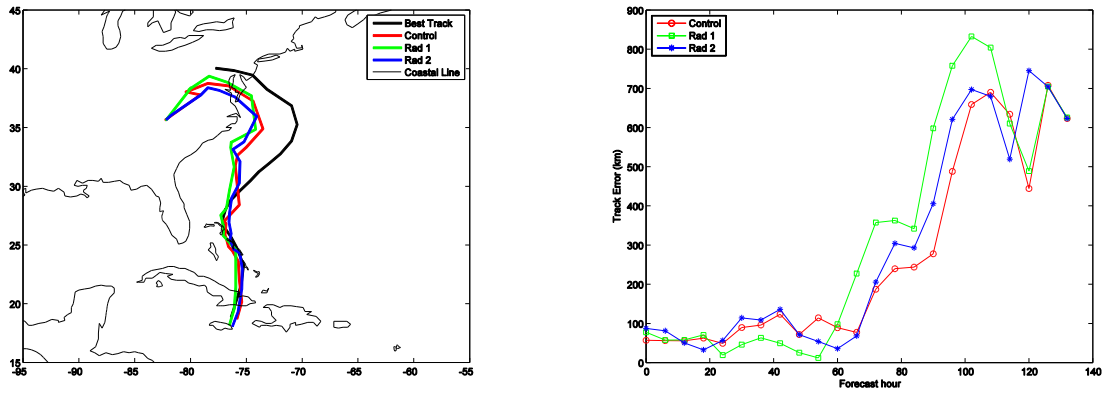


Figure 4: (left) Forecast tracks of the hurricane Sandy on 00 UTC 25 October 2012 for the different assimilation experiments. (right) The track error in km as a function of forecast hour for the different assimilation experiments.

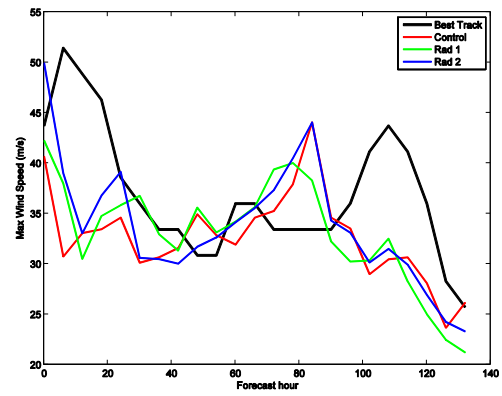
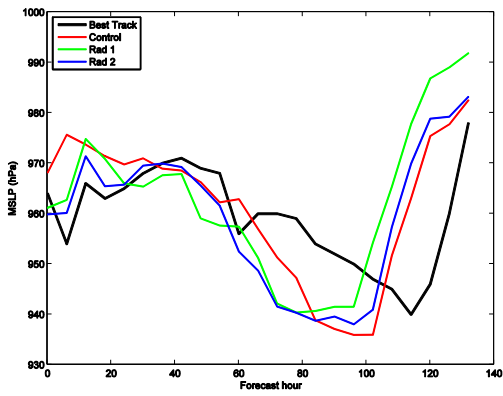


Figure 5: Minimum sea level pressure (left) and maximum wind speed (right) for the 132 h forecast period.

Table 1: AMSU-A and MHS channels characteristics.

Channel Number	AMSU-A Frequency (GHz)	MHS Frequency (GHz)
1	23.8	89.0
2	31.4	157.0
3	50.3	183.311 ± 1.0
4	52.8	183.311 ± 3.0
5	53.596 ± 0.115	190.311
6	54.4	
7	54.94	
8	55.5	
9	57.290	
10	57.290 ± 0.217	
11	57.290 ± 0.3222 ± 0.048	
12	57.290 ± 0.3222 ± 0.022	
13	57.290 ± 0.3222 ± 0.010	
14	57.290 ± 0.3222 ± 0.0045	
15	89.0	

Table 2: The datasets assimilated for the “Control” experimental run.

Observations	Platform
Upper air	sonde, aircraft
Land surface	synop, metar
Marine surface	buoy, ships
Satellite	geoamv, qscat